WARSAW UNIVERSITY OF TECHNOLOGY Index 351733
FACULTY OF CIVIL ENGINEERING
COMMITTEE FOR CIVIL AND WATER ENGINEERING
POLISH ACADEMY OF SCIENCES ISSN 1230-2945
DOI: 10.24425/ace.2024.148936
ARCHIVES OF CIVIL ENGINEERING
Vol. LXX ISSUE 1 2024
pp. 693–705

Research paper

Force analysis and treatments for Lidong tunnel of Renxin expressway crossing karst caves

Kai Zhu[1], Kui Zhang[2], Xiang-Dong Wu[3], Xiang-Ge Chen[4]

Abstract: There are several large karst caves at haunch part of the Lidong Tunnel during construction, together with inrush water due to high pressure within these caves. In light of it, this paper takes YK342+113 section as an example and adopts finite difference software FLAC 3D, so as to analyze tunnel deformation when crossing karst caves under six different working conditions, including with or without karst cave, before and after karst treatment, along with support locations. According to analysis results: First, the wall rock mainly had deformation at tunnel vault when evacuating at the third bench, which is a critical monitoring focus for tunnel construction; Second, karst cave treatment contributed to better conduct forces on both sides of wall rock, thus reducing vault settlement, while not affecting horizontal convergence and upturn of vaults; Third, treatment measures were proved to be effective in minimizing wall rock deformation by comparing deformation curves under different conditions; Fourth, after treatment measures, the angular points within the cave's chamber had stress concentration, which might cause secondary collapse. Field monitoring data revealed that the final settlement of the tunnel vault was relatively consistent with the numerical analysis results, with a distinct change in daily settlement after initial support construction. By integrating numerical analysis and field monitoring, the rationality of the karst treatment plan was fully verified, providing a valuable reference for similar projects.

Keywords: Lidong tunnel, deformation patterns, finite difference, karst caves, treatment measures, monitoring data, rationality

[1]Bac., Guangdong Nanyue Transportation Investment and Construction Co., Ltd, Guangzhou 510199, China, e-mail: zhukai202306@126.com, ORCID: 0009-0000-1385-5743
[2]Bac., Shenzhen Expressway Operation and Development Co., Ltd, Shenzhen 518110, China, e-mail: zhangkuipb@163.com, ORCID: 0009-0007-9285-7237
[3]Bac., Poly ChangDa Engineering Co., Ltd, Guangzhou 510620, China, e-mail: 805110846@qq.com, ORCID: 0009-0007-1913-9044
[4]MsC., Chongqing Jiaotong University, School of Civil Engineering, Chongqing 400074, China; State Key Laboratory of Mountain Bridge and Tunnel Engineering, Chongqing 400074, China, e-mail: 599126034@qq.com, ORCID: 0009-0002-6239-8774

1. Introduction

Tunnel construction in karst regions will bring numerous engineering challenges. Under karst condition, tunnels are subject to various factors including karstification degree and the relative location of caves with respect to the tunnels, which can significantly affect tunnel stability and greatly differentiate them from those constructed in non-karst areas. Currently, there are considerable researches devoted to cave tunnels, covering topics such as cave location, size, scale, filling material, inrush water types and wall rock stability. For example, based on inrush water mechanism, Feng Xuedong summarized three corresponding hazards and proposed a formula for calculating the thickness of rock layers as a key indicator [1]. Zhang et al. adopted finite difference methods and on-site monitoring tools to analyze how sizes and locations of lurking caves affect the stress-strain field around wall rock and its deformation [2]. Jia et al. utilized geological radar and advanced drilling techniques to accurately pinpoint karst structure locations, scale, and filling material characteristics of a highway tunnel in Guangxi province in China [3]. What's more, Fan et al. conducted mechanical response model experiments on water-rich, pipeline-shaped karst tunnels, so as to study the impact of the cavity location and water head height on the internal forces of the lining structure, and build a numerical model accordingly [4]. Taking LK28+284 karst cave section of the Zhoupan Tunnel as an example, Liu et al. used geological radar and engineering geologic analysis to evaluate the stability of cave surroundings, providing suggestions for vault cavity and body support treatment to ensure tunnel safety [5]. By analyzing the impact of caves on the stability of large-section road tunnels, Cui choose a combination of numerical simulation and on-site measurement to explore a safe distance between caves and tunnels [6]. Zhang and Qi adopted an intelligent positioning method for tunnel excavation working face, which can greatly shorten the measurement and positioning time, accelerate the project progress, reduce project risks, shorten the construction period, and reduce project costs [7]. Han et al. studied the composite concrete lining, increased the thickness of the sprayed concrete layer and changed the grid structure, which has a good effect on reducing the settlement of the arch crown [8]. Sauer et al. used the section M–N curve to determine whether the bearing capacity of the lining section meets the load effect [9]. Kaper et al. analyzed the application of steel fiber reinforced concrete (SFRC) segment in the durability design of lining structure combined with practical engineering [10]. Qiu et al. studied the influence of section size and material strength on the ultimate bearing capacity of section based on local bending test [11].

Despite relatively comprehensive researches on karst tunnels, there are currently no unified research methods of critical construction techniques for tunnels across large karst caves. Actually, current major methods include computer numerical simulation analysis [12–14], theoretical analysis [15–17], and model experiments [18, 19], with its own unique advantages and disadvantages separately. For instance, Pan et al. used model experiments and numerical analysis to reveal the displacement, stress, and seepage pressure changes in pressurized water caves during water sudden-inflows [20].

In this paper, key construction techniques for the Changda Highway Tunnel crossing a large karst cave were studied through both numerical simulation and monitoring data. The deformation patterns of the rock surrounding the cave both before and after treatment, along with the efficiency of treatment measures were analyzed, which can provide significant reference for similar engineering projects within China.

2. Project overview

The Lidong Tunnel of Renxin Expressway is a parted tunnel with a net clearance size of 14.75 × 5.0 meters. During actual excavation, the wall rock of the Lidong Tunnel in the karst section with abundant water is mainly of grade IV. Large karst caves (Table 1) appeared repeatedly in haunch part, accompanied by inrush water under high pressure, which seriously affected the supporting structure's stress of the ultra-large section tunnel.

Table 1. Cavity size distribution during construction

S/N	Length	Burial depth	Description
1	ZK343+723-713	50 m	A cave appeared on the left arch waist with a size of about 4 m (in the direction of the line) ×3 m (in the circumferential direction)
2	ZK342+355-365	140 m	A cave appeared on the right arch waist with a size of about 7 m (in the direction of the line) ×3.5 m (in the circumferential direction)
3	ZK342+455	160 m	A cave appeared on the right arch waist with a size of about 7 m (in the direction of the line) ×6 m (in the circumferential direction)

Dring the construction of the right tunnel entrance of the Lidong Tunnel at the pile location of YK342+113, a karst cave was on the left arch foot of the pilot tunnel while constructing the forepole surface (Fig. 1). The cavity diameter was about 1–2 meters, extending towards the center of the tunnel vault (Fig. 2).

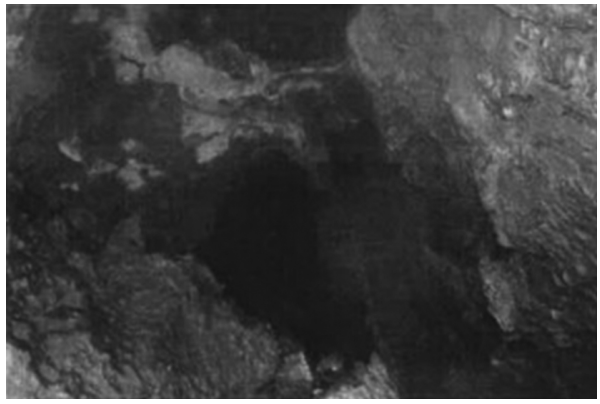

Fig. 1. YK342+113 Caves

Fig. 2. Tunnel support

3. Simulation analysis of tunnel karst cave construction

Based on field investigations and literature reference [11], the treatment plan for the sinkhole at the YK342+113 tunnel is illustrated in Fig. 3.

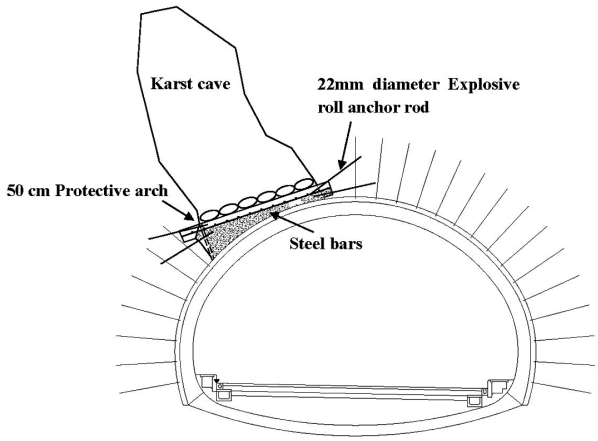

Fig. 3. Karst cave treatment of YK342 + 113 section

Steps are as follows:

1. In terms of protective arch, C25 concrete (Concrete with a compressive strength of 25 MPa) with 22 mm diameter steel bars were used with a 20×20 cm interval. Arch thickness should not be less than 50 cm. Meanwhile, the protective arch was embedded into the rock on both sides with a depth of no less than 50 cm to have higher stability.

2. The end of the protective arch was installed with 22 mm diameter explosive cartridge anchor rods with a length of 250 cm and a spacing of 1.0 × 1.0 m, along with a depth of no less than 1.5 min to wall rock.
3. A three-bench excavation method was adopted on site.

3.1. Modeling

Considering the location of the field karst, FLAC 3D numerical modeling was employed to analyze the deformation of the wall rock at the YK342+113 karstic section of the Lidong Tunnel, where the excavation span was about 17.21 m. The lining structure of this tunnel is illustrated in Fig. 4. For the arch wall section, C25 shotcrete (Concrete with a compressive strength of 25 MPa) with early strength was adopted, while I20b steel arch frames were installed with a spacing of 0.8 m. The invert arch and secondary lining were constructed with C30 (Concrete with a compressive strength of 30 MPa) concrete. The invert arch filling used C20 concrete backfill, which effectively reduced the weight of the tunnel and enhanced its overall stability.

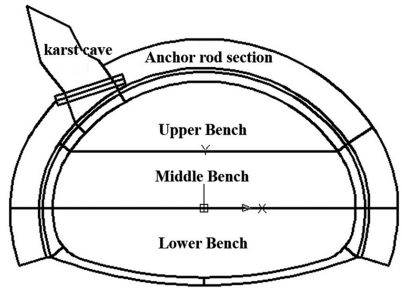

Fig. 4. Tunnel lining structure

Table 2. Initial support parameter

Shotcrete		Mesh reinforcement		Cartridge anchor rod			Steel frame	
Location	Thickness/ cm	Location	Mesh spacing/ cm	Location	Length /m	Spacing/m	Location	Spacing/ m
Arch wall	22	Arch wall	20 × 20	Arch wall	3.5	1.2 × 1.0 (Circum- ferential × longitudi- nal)	Arch wall	0.8

The basic dimensions and boundary conditions of the model are as follows:

1. The span of the double-line highway tunnel is D = 17.21 m.
2. To get more accurate calculation results, the distance on the left and right sides together with the bottom of the tunnel should be taken as 5D (generally 3–5D according to

research requirements of plastic zone's influence after tunnel excavation). The vertical height of the three-dimensional model was up to the ground surface (tunnel depth is 150 m), and the overall height of the three-dimensional model is 120 m, with the width of 160 m and longitudinal extension of 1 m, as shown in Fig. 5.

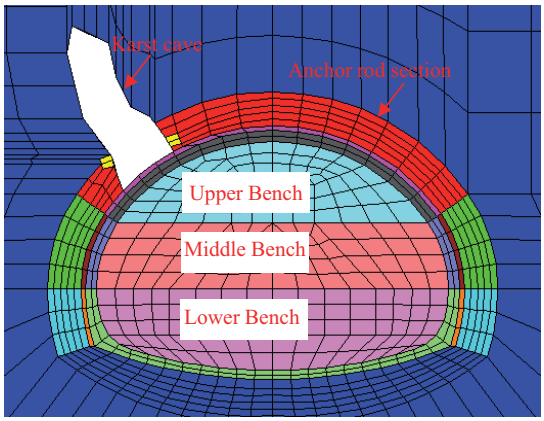

Fig. 5. Three-dimensional tunnel model

3. For the constitutive modeling of wall rock, the Mohr–Coulomb elastoplastic model is an alternative. When considering the support structure, the linear elastic material can be used to simulate the effects of shotcrete, anchor rods, and steel support structures.
4. During the numerical simulation, it is necessary to restrict the horizontal displacement in the normal direction and the vertical displacement at the bottom, and ensure that the top boundary is a free surface, thus ensuring the accuracy and reliability of the numerical simulation.
5. The simulation of the construction method is based on the three-bench excavation method.

Te simulated section is Grade IV wall rock assumed to be a single, homogeneous continuous medium, simplified as a uniform lithology. To simulate the effect of the anchor rods, higher parameters of wall rock can be utilized for equivalent simulation, but only with higher cohesion. Therefore, this calculation mainly considered safety aspect without the effect of pre-reinforcement. The physical and mechanical parameters for the calculation are shown in Table 3.

To get more precise stress calculations of the I20b steel arch, it is necessary to convert the longitudinal extension section into a modulus of elasticity and use it for initial support, which ensures calculation accuracy and support reliability.

$$E = E_0 + \frac{S_g \times E_g}{S_c} \tag{3.1}$$

where: E – comprehensive elastic modulus (Pa), E_g – elastic modulus of steel (Pa), E_0 – elastic modulus of shotcrete (Pa), S_g – cross-sectional area of the steel arch (mm^2), S_c – cross-sectional area of the shotcrete (mm^2).

Table 3. The physical and mechanical parameters of the surrounding rock structure

Items	Modulus of elasticity E (GPa)	Poisson's ratio μ	Cohesion E (kPa)	Frictional angle φ (°)	Density (kg/m^3)	Constitutive relation
Wall rock	3.0	0.3	300	30	2100	Mohr–Coulomb
Anchor rod area	3.0	0.3	390	30	2100	Mohr–Coulomb
Initial support	26.6	0.2	–	–	2300	Elasticity
Secondary lining	33.3	0.2	–	–	2500	Elasticity

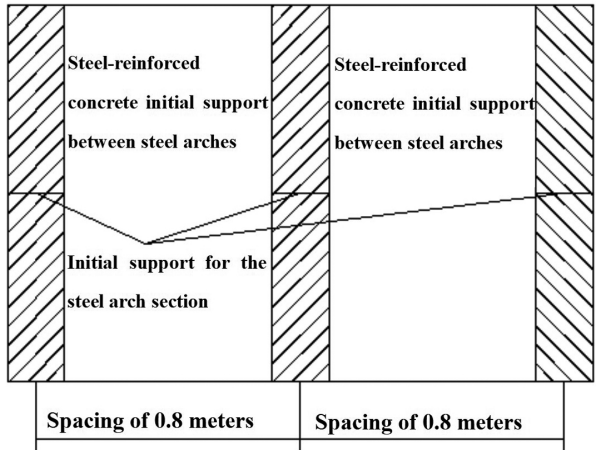

Fig. 6. Simplified schematic diagram of initial support sections

As illustrated in Fig. 6, the initial support for the steel arch section and the steel-reinforced concrete support for the segment between steel arches can be distinguished.

The simulation adopted a three-bench construction method. The process consisted of five construction stages as follows:

1. The upper steps of the target section are excavated and a cave support structure is constructed by modifying the model parameters.
2. The initial support of the upper bench was built on the target section.
3. The excavation of the middle step in the target section was carried out by deleting units, and initial support was provided for the middle step.
4. The excavation of the lower bench on the target section was executed, and the initial support of the lower step was constructed.
5. The excavation of the inverted arch commenced, and the initial support for the arch section was established. Finally, the initial support was closed, and convergence of the vault settlement was monitored.

In the calculation process, the displacement and stress changes for each construction stage were recorded, so as to better understand construction progress.

3.2. Calculations under various working conditions

In order to test support structure of the YK342+113 section by three-bench excavation, along with deformation and stress of wall rock, initial support and other structures, corresponding simulation calculations were conducted. In terms of specific calculations and analysis for six different working conditions, please refer to Table 4 for details.

Table 4. Calculations under various working conditions

Type of working conditions	Cave Condition	Support conditions
1	No cave	None
2		Initial support + anchored system
3	With cave (s)	None
4		Cave treatment
5		Initial support only
6		Cave treatment + initial support + anchored system

3.3. Analysis of calculation results

Six different construction conditions were analyzed, and the corresponding deformation curves of wall rock were shown in Figs. 7–9, the tunnel displacement under different working condition were shown in Fig. 10. These results highlight close monitoring and management of construction site conditions to ensure safe and effective tunneling operations.

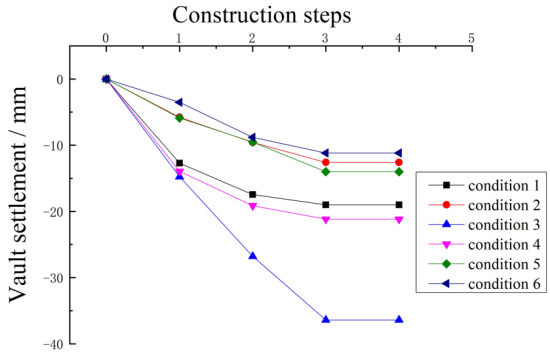

Fig. 7. Settlement curves of tunnel vault under different working conditions

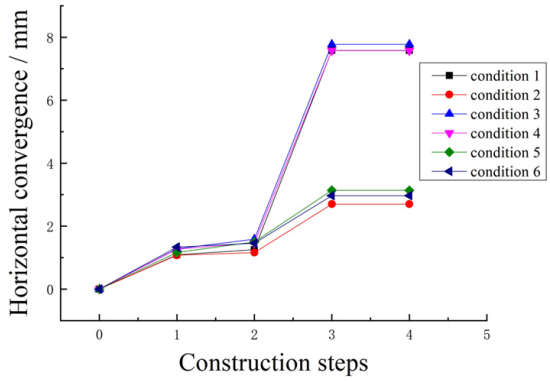

Fig. 8. Tunnel horizontal convergence curve under different working

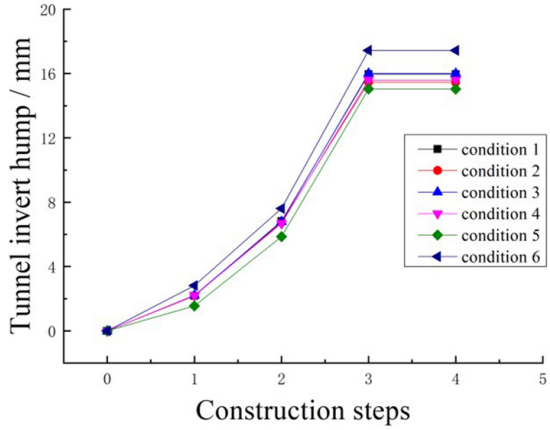

Fig. 9. Tunnel invert hump curve under different working condition

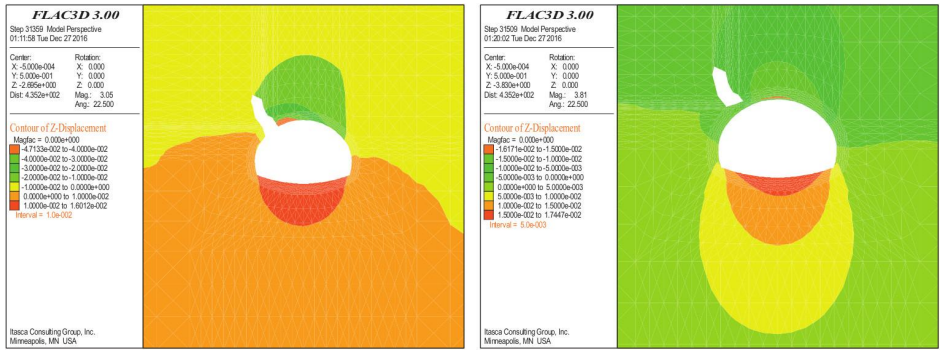

(a) (b)

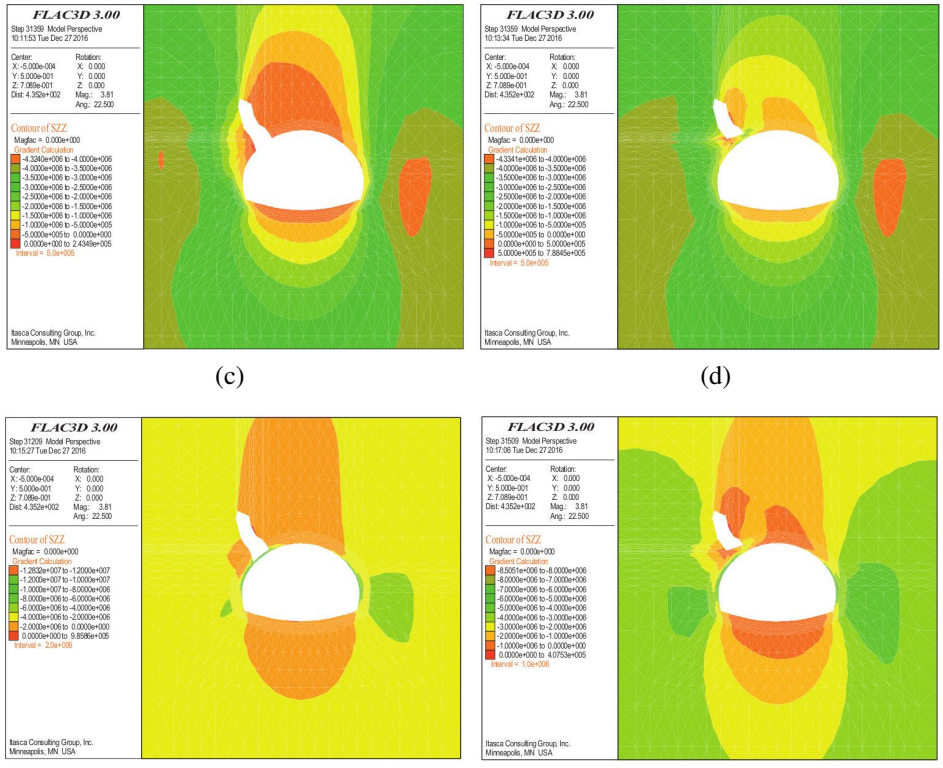

Fig. 10. Tunnel displacement under different working condition: a) 1, b) 2, c) 3, d) 4, e) 5, f) 6

Based on the observation of displacement curves of tunnel vault at different construction steps, if without any support, karst caves resulted in vault settlement of 36.4 mm, while maximum vault settlement was only 19.0 mm without karst caves.

During the initial excavation, vault settlement rate increased rapidly, but gradually stabilized as this stage progressed. Analysis of the accumulated settlement of the tunnel vault beneath karst caves comes to following results: Working condition 3 had the most severe vault settlement, followed by working conditions 4, 5, and 6. As supporting structures for the tunnel were strengthened, the cumulative deformation of the vault gradually decreased, which effectively mitigated the risk of vault settlement.

Under working conditions 1, 3, and 4, there were evident changes in the horizontal convergence, with curves that appeared quite similar to each other. It indicates that karst caves have relatively low influence on tunnel's horizontal convergence. Conversely, under working conditions 2, 5, and 6, horizontal convergence has relatively small changes with curves that are almost identical. This suggests that initial support has significant influence on horizontal convergence of the tunnel.

Based on the numerical analysis, vertical stress contour maps of the tunnel wall rock were obtained for these six different working conditions, which demonstrate as follows:

1. Without support structures, stress concentration and large settlement occurred at the intersection between the tunnel and karst caves, leading to instability. Appropriate treatment is necessary to address this issue.
2. After treatment and the installation of support structures, the wall rock on both sides of karst caves was connected, ensuring balanced stress distribution for entire tunnel structure. The tunnel structure experiences better stress balance compared to situations without treatment.
3. With treatment plus systematic anchor rods and initial support, the tunnel structure enjoyed even better stress distribution and higher safety.

3.4. Conclusions from analysis

Based on the above simulation analysis, the following conclusions can be drawn to guide subsequent construction and monitoring:

1. During the three-bench evacuation process, a tunnel with a large three-lane section was excavated for a highway. The deformation of the wall rock was primarily manifested as vault settlement. Therefore, paying special attention to vault settlement with stronger monitoring is crucial in this process.
2. Through treatment structures, forces could be effectively transferred between the wall rock on both sides, thus ensuring the stability of wall rock and reducing vault settlement. To be noted, the influence of the treatment structure on the horizontal convergence and the invert hump were negligible. Therefore, karst cave treatment structures are feasible to ensure tunnel stability and effectively reduce vault settlement.
3. The results indicate that the treatment measures for karst caves in this tunnel are reasonable in ensuring the stability of the wall rock and thus reducing deformation.
4. After dealing with karst caves around the tunnel, it is vital to pay attention to stress concentration at the corners inside the karst caves as it can potentially cause secondary collapses inside the caves, endangering the safety of the tunnel lining structure.

4. Monitoring data before and after treatment

Based on on-site monitoring data, the vault settlement and surrounding convergence values of the YK342+114 section have been collected and depicted in Fig. 11. There was vault significant settlement before the completion of initial support, with a maximum daily settlement of 9 mm and a maximum change rate of 2.25 mm/d. After support installation, the daily settlement greatly reduced to a maximum settlement of 2 mm. The total final vault settlement during the monitoring period was 22 mm. That is, due to a sound stress system after completing the initial support, the treatment measure showed apparent effect, which is in accordance with the results of numerical analysis.

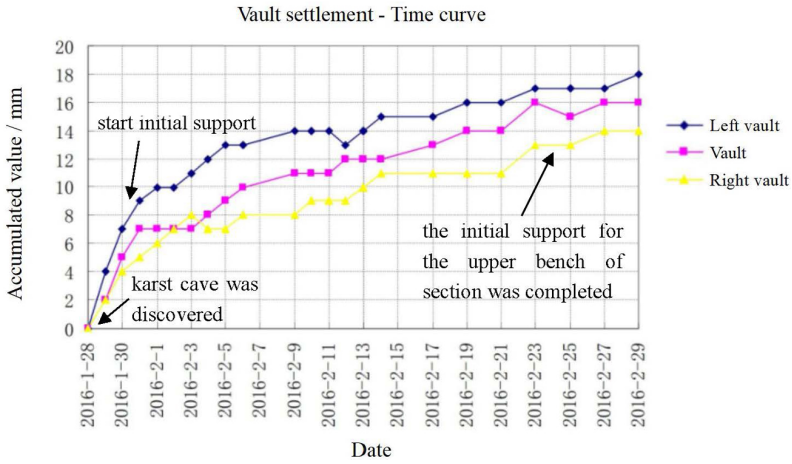

Fig. 11. Vault Settlement – Time Curve

5. Conclusions

Based on the treatment measures conducted at the karst cave located at YK342+113 of the Lidong Tunnel on Renxin Expressway, a numerical simulation was carried out. The analysis results are as follows: 1) Adopting the three-bench excavation method, the wall rock mainly had vault settlement and deformation, which requires monitoring of tunnel construction. 2) Treatment measures of karst caves could ensure better force transfer to both sides of the wall rock, which was crucial in reducing vault settlement. 3) According to comparisons of the deformation curves under different conditions, relevant treatment measures for karst caves were feasible in significantly reducing wall rock deformation. 4) After treatment, stress concentration at the corners inside the cave should be noted. To ensure the safety of the tunnel lining structure, appropriate measures should be taken inside the cave to avoid secondary collapses.

In conclusion, the final vault settlement values collected by on-site monitoring and numerical analysis were consistent. After installing initial support, daily settlement changed significantly. The combination of numerical analysis and on-site monitoring effectively verified the rationality of karst cave treatment measures and provided a reference for similar projects.

References

[1] X. Feng, X. Zhou, and Y. Hu, "Research progress in water inrush mechanisms of tunnels in karst area", *Journal of Wuhan Institute of Technology*, vol. 44, no. 3, pp. 250–259+354, 2022, doi: 10.19843/j.cnki.CN42-1779/TQ.202107020.

[2] J. Zhang, Z. Xia, X. Liu, J. Wang, X. Jiang, and F. Chen, "Numerical analysis on influence of concealed karst cave on tunnel excavation stability", *Science Technology and Engineering*, vol. 22, no. 13, pp. 5455–5462, 2022.

[3] J. Jia, D. Wang, Z. Zeng, and F. Qin, "Exploration of karst detection and construction treatment technology for large section highway tunnels", *China Water Transport*, vol. 2022, no. 4, pp. 121–124, 2022, doi: 10.13646/j.cnki.42-1395/u.2022.04.040.

[4] H. Fan, D. Zhou, Y. Liu, Y. Song, Z. Zhu, Y. Zhu, X. Gao, and J. Guo, "Mechanical response characteristics of lining structure of pipeline karst tunnels in water-rich areas", *Rock and Soil Mechanics*, vol. 43, no. 7, pp. 1884–1898, 2022.

[5] G. Liu, C. Shi, D. Xu, X. Huo, H. Du, and F. Yang, "Stability analysisnand mitigation measures of karst rock cavities surrounding Zhoupangou tunnel", *Soil Mechanics and Foundation Engineering*, vol. 36, no. 1, pp. 12–15, 2022.

[6] H. Cui, "Karst cave versus large section highway tunnel study on the influence of surrounding rock stability and safe distance", M.A. thesis, Anhui University of Science and Technology, Huainan, 2021.

[7] J. Zhang and Y. Qi, "Research on the intelligent positioning method of tunnel excavation face", *Archives of Civil Engineering*, vol. 68, no. 1, pp. 431–441, 2022, doi: 10.24425/ace.2022.140178.

[8] W. Han, T. Xiao, D. Shi, and Y. Wang, "Optimization of heavy haul railway tunnel lining based on ultimate bearing capacity", *Archives of Civil Engineering*, vol. 68, no. 4, pp. 493–511, 2022, doi: 10.24425/ace.2022.143051.

[9] G. Sauer, V. Gall, and E. Bauer, "Design of tunnel concrete linings using limit capacity cures", in *The 8th International Conference on Computer Methods and Advances in Geomechanics*. 1994, pp. 22–28.

[10] T. Kasper, C. Edvardsen, G. Wittneben, and D. Neumann, "Lining design for the district heating tunnel in Copenhagen with steel fibre reinforced concrete segments", *Tunnelling and Underground Space Technology*, vol. 23, no. 5, pp. 574–587, 2008, doi: 10.1016/j.tust.2007.11.001.

[11] Y. Qiu, K. Feng, C. He, L. Zhang, and C. Wang, "Investigation of the ultimate bearing capacity of a staggered assembly segmental lining for an urban gas transmission tunnel", *Sustainable Cities and Society*, no. 48, pp. 1–13, 2019, doi: 10.1016/j.scs.2019.101551.

[12] G. Xiao, Y. Li, and Q. He, "Construction and treatment technology for karst caves through the arch of highway tunnel engineering", *Building Technology Development*, vol. 49, no. 10, pp. 105–109, 2022.

[13] Y. Chen, C. Wang, M. Guo, and P. Lin, "Influence of concealed karst cave on surrounding rock stability and its treatment technology", *Journal of Shandong University (Engineering Science)*, vol. 50, no. 05, pp. 33–43, 2020.

[14] J. Huang, T. Xie, J. Chen, Y. Qian, and S. Song, "Influence analysis of karst cavity on tunnel stability", *Construction Technology*, vol. 47, no. 14, pp. 25–28, 2018.

[15] Z. Wang, D. Chen, Z. Ye, B. Sun, and J. Zhang, "Treatment technology of karst cave in mountain tunnel", *Highway Engineering*, vol. 41, no. 02, pp. 72–74+112, 2016.

[16] J. Guo, H. Li, F. Chen, and Z. He, "Theoretical analysis on water-resisting thickness of karst tunnel face", *Chinese Journal of Underground Space and Engineering*, vol. 13, no. 05, pp. 1373–1380, 2017.

[17] S. Wang and H. Deng, "Study on deformation law of surrounding rock of karst tunnel based on SPSS", *Construction Technology*, vol. 45, no. 13, pp. 125–129, 2016, doi: 10.7672/sgjs2016130125.

[18] X. Tan, H. Fan, Y. Song, Y. Liu, and H. Yang, "Experimental study on the mechanical characteristics of the lining structure of pipe-type karst tunnel", *Chinese Journal of Underground Space and Engineering*, vol. 17, no. 06, pp. 1847–1856, 2021.

[19] S. Deng, A. Hong, Z. Xu, and P. Lei, "Experimental study on water inrush duration characteristics of filling-typed concealed karst cave in karst tunnel", *Water Resources and Hydropower Engineering*, vol. 52, no. 5, pp. 97–108, 2021, doi: 10.13928/j.cnki.wrahe.2021.05.011.

[20] D. Pan, S. Li, Z. Xu, L. Li, W. Lu, P. Lin, X. Huang, S. Sun, and C. Gao, "Model tests and numerical analysis for water inrush caused by karst caves filled with confined water in tunnels", *Chinese Journal of Geotechnical Engineering*, vol. 40, no. 05, pp. 828–836, 2018.

Received: 2023-05-21, Revised: 2023-11-14